Cleaner Engineering and Technology 6 (2022) 100390

Contents lists available at ScienceDirect

Cleaner Engineering and Technology

journal homepage: www.sciencedirect.com/journal/cleaner-engineering-and-technology

In-depth exploration of partial discharge modelling methods within insulations

Hadi Nabipour Afrouzi [a,*], Ateeb Hassan [a], Daphne Tay Ye Chee [a], Kamyar Mehranzamir [b], Zulkurnain Abdul Malek [c], Saeed Vahabi Mashak [c], Jubaer Ahmed [d]

[a] Faculty of Engineering, Computing and Science, Swinburne University of Technology Sarawak, 93350, Kuching, Malaysia
[b] Department of Electrical and Electronic Engineering, Faculty of Science and Engineering, University of Nottingham Malaysia, Jalan Broga, 43500, Semenyih, Selangor, Malaysia
[c] Institute of High Voltage & High Current Faculty of Electrical Engineering Universiti Teknologi Malaysia, Johor Bahru, 81310, Malaysia
[d] School of Engineering and Built Environment, Edinburgh Napier University, Merchiston Campus, 10 Colinton Road, Edinburgh, EH10 5DT, UK

ARTICLE INFO

Keywords:
Partial discharge
Simulation and modeling
Cavity
Insulation
High voltage

ABSTRACT

Partial discharge (PD) activities are the essential contributor of insulation failure, which constitute more than 60% for damaging high voltage equipment. This article presents a critical review on the modelling of partial discharge using different techniques. Monitoring partial discharge activities is essential to enhance the comprehension on the phenomena of partial discharge through modelling process. A lot of tools have been introduced to assist PD measurement in diagnosing and monitoring the condition of high voltage insulation system. This article will evaluate the development of important PD models such as three-capacitance model, Pedersen's model, Finite Element model (FEA), and Niemeyer's model. This review attested that the research studies done on partial discharge are still deficient and there are still countless of study on partial discharge to be carried out. The parameters that have influence on partial discharge occurrence inside cavities in solid dielectric materials are statistical time lag, inception field, effective charge decay time constant, and cavity surface time constant. The initial free electron required for the existence of a PD is provided by the electron surface emission and volume ionization with the cavity while applied voltage's amplitude and frequency are the stress conditions affecting PD behavior in cavities as well as cavity's size, shape, and location. A Comparison regarding modeling time and accuracy of the model between different models of partial discharge have been done in this article. From where it can be concluded that the FEM and Niemeyer's model are suitable for PD due to their average cost and low degree of application, but FEM is commonly used because it is more accurate and easiest model. Moreover, from a comparison of advantages and limitations of different models, it is shown that FEM model has one major limitation that the large amount of data is required during meshing process. Besides, Niemeyer's model is not accurate due to the fundamental assumptions made and these assumptions are not clearly justified with high reliance over immeasurable free parameters.

1. Introduction

Degradation of insulation system is a primary constraint in electrical power system pertaining to high voltage equipment and machineries. Insulation deterioration can result in unforeseen failures in the electrical power utilities, inducing prolong downtime and high maintenance costs. Different methods of investigating partial discharge are introduced in diagnosing insulation failure. The most prevalent method used is phase-resolved partial discharge (PRPD) representation, until a more advanced method, pulse sequence analysis (PSA) has arrived as a substitute in 1990's (Aziz et al., 2017).

Partial discharge exists in an electrical insulator during the presence of high electric field stresses, under the condition where no connection is established between the electrodes (Hussain et al., 2021). A lot of research on PD in solid dielectric system, specifically in air gaps and cavities has been conducted over the years with published papers to enhance the comprehension on partial discharge principle through in-depth elucidation of partial discharge phenomena. The simulation

* Corresponding author.
E-mail address: HAfrouzi@swinburne.edu.my (H.N. Afrouzi).

https://doi.org/10.1016/j.clet.2021.100390
Received 17 May 2021; Received in revised form 25 December 2021; Accepted 31 December 2021
Available online 4 January 2022
2666-7908/© 2022 The Author(s). Published by Elsevier Ltd. This is an open access article under the CC BY-NC-ND license (http://creativecommons.org/licenses/by-nc-nd/4.0/).

works on cavities exist in solid insulation material agrees with the experimental results and it has proven the factor of insulation degradation in high voltage utilities, which is the partial discharge. Whence, extensive knowledge on the behaviors of insulation under operational stresses will contribute to accurate prediction of the insulation failure (Adam and Tenbohlen, 2021). Apart from that, modelling of partial discharge phenomena in electrical insulators will also aid in understanding the progression of PD and concurrently interpreting features of PD pattern (Niasar et al., 2021).

However, it is difficult to model and design the physical phenomenon of PD due to differences between modelling and actual demands of observable and realism (Afrouzi, 2015). Nevertheless, modelling and simulating partial discharge occurrence do provide an alternative way in investigating partial discharge activities while inspecting the influence of critical parameters such as the size and location of cavities, applied voltage, type of insulation material used and cavity's gas pressure on PD behavior (Pan et al., 2020). The study on the effects of the pivotal parameters on partial discharge activities is crucial to improve the precision as well as the dependability of PD diagnosis (Gouda et al., 2018).

Pulse Height Analysis and Phase Resolved Measurement techniques in observing distinctive PD patterns are two of the methodologies introduced for PD identification by Rodríguez-Serna et al. (2020) and Ali et al. (2018). Moreover, Majidi et al. (2015) asserted that electrical discharges are contributory on emitting gaseous by products such as Ozone, O3 and Nitrogen gases. On that account, through analyzing the decomposed gases in air from the electrical discharges will assist the detection of DBD (Dielectric Barrier Discharge) (Suzuoki et al., 1996). One of the methods that has been introduced by Shcherbanev et al. (2016) to analyze PD gaseous products emission is emission optical spectroscopy. Emission spectroscopy is used in estimating the density of the emitted gaseous while identifying the exact chemical composition of the gas based on the spectrum of PD resolved emission and its corresponding shapes of pulse throughout the entire aging process of the insulation system (Li et al., 2017a,b).

The tree shape structure, known as the electrical trees, signifies the stage before the incidence of electrical breakdown within high voltage insulation network. The occurrence of PDs is induced by the expansion of the electrical tree branches (Lv et al., 2018). A few characteristics that help to distinguish the form of discharges are the magnitude, number of occurrences per power cycle, patterns per resolved phase, and their dependency on the voltage applied. In reference to the plot generated on the ratio of accumulated damage against the zone radius, the growth of electrical trees can be divided into three stages: initiating, stable growth, and finally uncontrolled growth stage (Kaneiwa et al., 2000). According to previous research studies, the fine tree growth, fast forward growth, tree channel propagation, conception, and reverse tree growth are phases in which the entire tree process should be divided. At these different stages of treeing progress, the PDs are exhibiting different characteristics and the changes in the characteristics of partial discharges are noticed to be in parallel with the distinct phases of electrical tree growth. Suzuoki et al. (1996) designed the feigned defects as long single channels inserted inside polyethylene insulation material to analyze the alteration in the characteristics of PD in corresponding to electric tree propagation. Based on their findings, the size of the feigned defect has a major influence over determining the pattern of PD resolved with phase.

The PD pattern exhibits a wing-like shape in long narrow channels (Yang et al., 2021), which also resembles a tree of electrical branch (Lv et al., 2017). While the PD pattern show to be alike as turtle or rabbit shape in short or wide channels, resembling the shape of a cavity (Alsheikhly and Kranz, 1991). Fig. 1 shows the previously described distinguishable forms of PD pattern; the wing-like and turtle like PD.

2. Different types of modelling techniques

All the modelling techniques discussed in this section had been applied in modelling PD from cavities that had been surrounded by solid material. The capacitance model will not be reviewed in this work since it has been reviewed largely by the other researchers.

2.1. Finite element model for partial discharge modelling

The disruption in the electric field is numerically resolved since the discharge in the cavity dielectric material is designed using FEA. The subdomain and boundary parameters are assigned before the model is solved. The benefit of utilizing FEA to analyze PD occurrence is that pre-discharge event is learnt by obtaining field interruption figures. Additionally, the impact of electrode and the surface charge dispersion across the wall of the cavity gives rise to irregular electric field disruption in the cavity, which can also be modelled using FEA. Apart from that, the temperature and electric field can be obtained simultaneously by introducing Multiphysics' specifications to the model. The downside of employing FEA in partial discharge modelling include a long simulation time due to the meshing procedure, which necessitates fine-tuning on the problematic section for better and more accurate results.

The electric current and electrostatic models are two FEA methods of modelling PD occurrences. Fig. 2 represents the 2D geometry of electric current FEA model while Fig. 3 shows 2D geometry of electrostatic FEA model.

The determining equation used in solving the electric potential for the electric current model (Illias et al., 2017) is given below.

$$-\nabla\cdot(\sigma\nabla V) - \nabla\cdot\frac{\partial}{\partial t}(\varepsilon\nabla V) = 0 \tag{1}$$

Where the permittivity is represented as ε , the electric potential is defined as V and the electrical conductivity is expressed as σ.

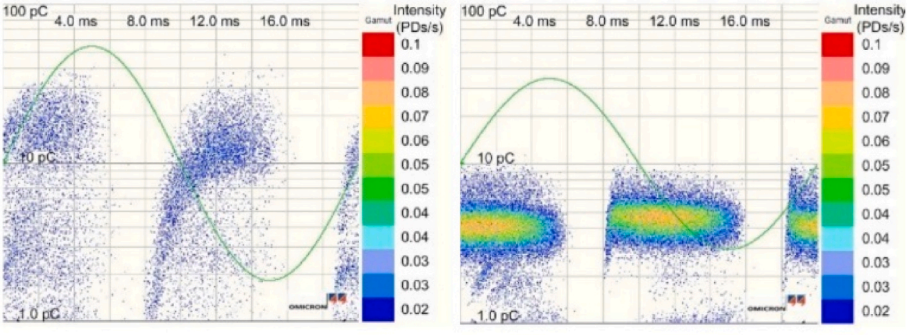

Fig. 1. Distinguishable forms of PD patterns (a) wing-like PD (b) turtle-like PD (Lv et al., 2017).

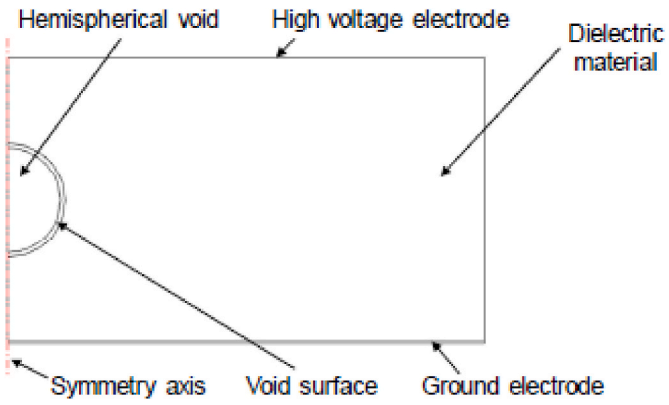

Fig. 2. The FEA model of electric current in 2D geometry (Illias et al., 2017).

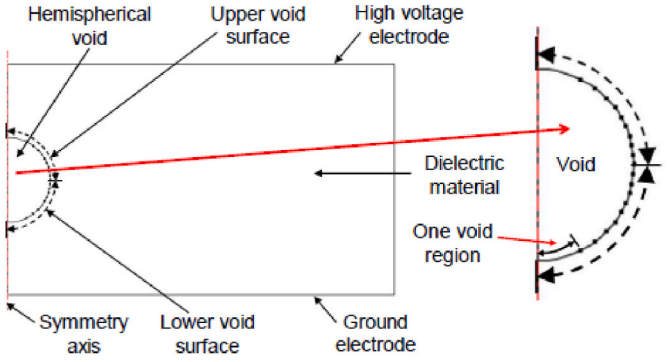

Fig. 3. The 2D geometry of electrostatic FEA model (Illias et al., 2017).

In the partial discharge simulation in a cavity using an electric current FEA model, the 2D geometry of the electric current FEA model in the above figure is used. To model the reduction of charge via surface conduction, this model includes a hemispheric cavity formed by an axially symmetric, homogeneous dielectric material, and a cavity surface.

This model assumes that discharge occurs along the cavity's symmetry axis. It is also assumed that discharge affects the entire cavity during the discharge process, causing the conductivity σ_{cav} of the entire cavity to rise from a small value to a higher value. Ergo, cavity's electric field, E_{cav} is reduced and σ_{cav} resets to an inferior value as E_{cav} goes below the extinction field. E_{ext}.

The electric current model in FEA enables for dynamic modelling of PD current over time. As a result, the cavity's PD pulse current I_{PD} can be obtained. The current integration method can be used to calculate the partial discharge apparent and real charge magnitudes via the ground electrode as well as center of the cavity during a discharge duration. Equation (2) is used to calculate the charge regarding to partial discharge occurrence.

$$q_{PD} = \int_{t}^{t+dt} I_{PD} dt \tag{2}$$

Since it is estimated that the partial discharge afflicts the entire cavity, the non-uniformity of electric field cannot be modelled in the surface charge dispersion across wall of the cavity, but in the electric current model.

Apart from that, the electrostatic model can be used to model PD occurrences in a cavity using the FEA method (Kai et al., 2007). In this model approach, the assignment of conductivity values is no required since there is no current involved, thence, the number of parameters is reduced as compared to the electric current model in FEA method. The equation relating to the electric field dispersion in electrostatic model is

$$\nabla \cdot \varepsilon E = 0 \tag{3}$$

The 2D geometry of an electrostatic FEA model with a hemispherical chamber and insulation material is shown in Fig. 3. The surface charge distribution on the cavity wall controls the electric field inside the cavity (Kai et al., 2004). Ergo, it is not required to assign the cavity surface as a subdomain. There are 10 identical area regions modelling the uppermost and lowermost cavity surface to design the charge distribution on the wall's cavity (Illias et al., 2014).

The simulation time and electric field calculation proved reasonable and accurate results sequentially, when the cavity regions were divided into 10, after various testing (Illias et al., 2013). However, a division of a higher number of regions resulted in a longer simulation time whereas the electric field calculation in the software proved better accuracy. Alternatively, a division of lower number of regions resulted in the opposite effect (Crichton et al., 1989).

The PD is projected to occur outside of the cavity surface on the axis of symmetry, stretching via the cavity across the axis of symmetry, and reaching the other side of the cavity wall as the discharge occurs. It is considered that across the cavity wall, the charges are spread once the partial discharge charges reach the cavity wall (Pedersen et al., 1991). Increasing the charge density on the wall's cavity ($\rho s0$), conducts the modelling of discharge event, where charges propagate with $\rho s0$ until the net electric field along the void axis of symmetry E_{cav} goes below the extinction field E_{ext}.

The magnitudes of the PD apparent and real charges are not computed using the analytical method, even though this model utilizes the theory of induced charge because of a PD. In fact, the FEA concept calculates charge magnitude numerically based on the charge distribution on the cavity wall following a discharge. The numerical technique is an additional benefit of using this model when compared to the analytical and FEA approaches. Though, it is hard to decide the charge motion via conduction across the cavity surface as consideration needs to be established on the speed of charge movement from its original deposited location on the cavity wall to the other location across the cavity wall. Moreover, the electrostatic model of FEA method has a disadvantage when it comes to the prediction on the distance of charge propagation across the cavity wall when the charge reaches the cavity wall throughout discharge occurrence.

A new method for simulating discharge processes in dielectric breakdown was provided by Noguchi et al. (2020), which incorporates field fluctuations based on Maxwell's equation in the finite element framework but does not use artificial stochastic disturbance. These equations assume that when electrical treeing develops, field fluctuations act as electromagnetic waves and set off the next dielectric breakdown. The resulting model can be viewed as an equivalent circuit model, with the resistors located on the Delaunay edges as in the real circuit. The conductivity and shape of the local mesh influence the resistance values of these resistors.

Because resistance levels are determined independently of one another in their model, the dielectric breakdown can be described as the replacement of resistors. This can be depicted numerically as a change in local conductivity values or functions. Besides, the choice of unstructured meshes was shown to implicitly include stochastic features into the discretized model. Due to this capability a Monte-Carlo simulation can be run by just altering the domain decomposition. However, the computing cost and accuracy must be carefully discussed, whence the Monte-Carlo simulation by using the proposed method could be one of the feasible approaches for predicting stochastic dielectric discharge processes. A numerical analysis was also performed for three-dimensional discharge patterns, but it has certain limitations due to the assumption of a uniform initial charge density distribution and several parameter settings such as conductivities before and after breakdown and breakdown voltage. As a result, for a more realistic simulation, the initial charge density distribution as well as more exact

parameter setting must be considered.

The samples of a study into the surface discharge behavior of several dielectric samples under DC was presented by Madhar et al. (2021). It builds a knowledge base for the study and analysis of partial discharge (PD) defects in a linear fashion with the goal of identifying PD defects under DC. The dielectric's material properties are measured to make this possible. The electric field and dielectric parameters that affect partial discharge behavior are estimated using a finite element (FEM) simulation. Based on simulation results and other literature, the DC-PD experiments conducted on surface dielectric samples shows a highly realistic behavior. This study concluded with the presentation of new partial discharge fingerprints for the surface PD fault, which will aid in defect detection under HVDC.

Moreover, Chalaki et al. (2021) conducted a study to classify and compare AC and DC partial discharge based on PD pulse waveform analysis. A testbed was created to fulfil this goal, allowing for exact measurements of individual PD pulses. The testbed is used to collect data from four different types of PDs created by individual PD source samples: cavity, surface, corona, and floating potential discharges. Thousands of PD pulses were collected by examining all samples under AC, positive DC, and negative DC electrical stresses. Following that, each PD type's waveforms were divided into representative groups based on their discharge mechanisms. The statistical data from the recorded pulses was used to distinguish between AC and DC PDs, while the clustered patterns of PD amplitude versus their temporal properties were used to categorize the different types of PDs under AC and DC electrical stresses.

In addition, benefit of using this mapping method under DC stress is its independence from the repetition rate information provided by PD pulses. This method takes a long time to record data and is widely used in TRPD research. Another benefit of this method is that each of the rise time, decay time, and pulse width of PD waveforms can be used to identify and cluster the data. Finally, other probable properties of PD waveshapes, such as their integral (area under waveform) can be examined in future research to classify varieties of PDs by considering the time characteristics of produced PD pulses.

2.2. Niemeyer's model for partial discharge modelling

Niemeyer's model is known to be the fundamental for most of the current literature on PD modelling. In Niemeyer's model, he introduces two settings that encourage the occurrence of PD, which uses computer simulation to track each step time. The electric field inside the cavity is presumed to be constant and the partial discharge q_{app} is calculated using the derived equations from a former analytical study of Crichton et al. (1989).

The inception condition is deemed as deterministic, disregarding whether the field is attainably high enough for PD occurrence while having comparison done between the magnitude of the electric field in cavity and value of electric inception at each stepping time. The electric inception field is highly liable on the size of the cavity considering of the discharge direction and gas pressure (Gross, 2018).

In an air-filled cavity, the formula of electric inception field is retrieved from the work of McAllister and Pedersen (1981). Referring to this work, the equation of inception field is then derived based on measurements of electrical breakdown between the metallic parallel electrodes plate, although its application on air filled cavity with surrounding dielectric layer are raising uncertainty. Once a discharge has transpired, it is deduced that the electric field will decrease until it reaches a residual value, E_{res} which is subjected to the gas pressure within the cavity. In this scenario, the E_{res} is set to the value that corresponds to the electric field in the streamer's discharge channel (Höfer and Berger, 2018).

But clarity is lacking for the justification on this work where it is more equitable in assuming that the charge recombination in the gas and the accumulation of surface charges at the dielectric boundaries would alter the electric field following the discharge process (Nijdam et al., 2010). Apart from that, the electric field in a needle-plane system is probably determined by the streamers between the metallic electrodes, which is not a practical representation of majority environments of the PD systems (Hikita et al., 2010).

In dielectric bounded cavity, the surface emission occurs in the event of returning charge delivered by the earlier PDs emitted back inside the cavity (Villa et al., 2017). The activation of this process happens after the first PD occurrence in the cavities and the free electrons are presumably generated in the cavity attributable to radiation from the background. Since long inception delay is commonly detected before the initial PD occurrence, it is deduced that the background radiation during this period is very low which instigate surface emission to be the dominant mechanism of generating free electrons for discharges (Castro et al., 2016).

Apart from that, an equation that is prevalently used to govern the electron production rate from surface emission, $\dot{N}_{es}$ for surface of insulator is shown as below.

$$\dot{N}_{es}(E_v,\ N_{dt};\ T, \Phi) = V_0 N_{dt} \exp\left(\frac{1}{k_B T}\left[\sqrt{\frac{e^3|E_v|}{4\pi\varepsilon_0}} - \Phi\right]\right) \tag{4}$$

where V_0 represents the fundamental phonon frequency, N_{dt} is the number of electrons presents in disengaging traps at the surface. E_v, is the electric field inside the cavity, Φ is an effective work function and T is the temperature. Niemeyer model is implemented on the consideration that, the number of electrons in disengaging traps, N_{dt} will be equivalent to the sum of amount of the electrons used by the discharge inside the dielectric surface at that instant moment right after the discharge. The period between the discharges displayed an exponential decay. Anyhow, there is no physical evidence to support the assumptions made on this model with the presence of limited understanding on the rate of electron generated from trapped charge in insulators. Besides, it is noticeable that the results from the modelling work are significantly reliant on both Φ and the time constant that presides over the decay of N_{dt}, with both being regarded as free parameters that are readjusted to fit into experimental data (Li et al., 2017a,b).

On the other hand, detailed literature review has uncovered the inconsistencies of this equation. This is attested as Schottky term is not included in the origin of Niemeyer's work. Again, the progression of equation (4) can be traced back to a proposed equation from the early work explaining the rate of electron generation initiated by the deposition of surface charge owing to discharges event between vacuumed concentric glass tubes ((McAllister and Pedersen, 1981). Apart from that, the previous work has used Schottky term with a magnitude that is two times larger due distinct methods applied on the potential of electron. The investigation of the potential of electron in Schottky term is carried out in relation to the images attained at the metallic boundary whereas the potential of electron at the dielectric boundary is inspected at the space between an electron and a void (Iddrissu et al., 2018).

The divergence of these two methods applied would not significantly affect the previous results employing Equation (6). However, the equation corresponding to the methods applied are found fallacious after thorough literature study. This is because the consideration of surface emission from metallic surfaces places an assurance over Niemeyer proposal, which stated the possibility of numerous surface emission processes, inclusive of ion impact, which comply with the thermionic emission law scaling of Richardson-Schottky. This is highly erroneous as thermionic emission is negligible for temperatures applied in most investigated PD systems of interest, and so there is no supporting evidence ascertains that the same scaling technique can be applied in fundamentally distinctive physical processes.

Simulations performed based on this model has given accurate results which agree with the PRPD patterns for epoxy bounded spherical cavities under varying conditions. The Morshuis and Kreuger (1990) has reasoned that the application of this model is highly extensive towards

wide ranging gaseous defaults bounded by solid dielectric by providing the supporting look up table for fifteen different defects that can be configured using this model in (Zeng et al., 2019; Hermansyah et al., 2018).

Nevertheless, this model has only been applied to an epoxy bounded spherical air-filled cavity and an electrode protrusion in SF6 (Seghir et al., 2006). The model is applied to assist the investigation on the changes in PRPD patterns owing to corresponding discharge event over extended time length ((Daphne et al., 2019a). In this experiment, to reproduce the standardized 'rabbit ear' discharge patterns, a scaling factor is applied to equation (5) with the reasoning that adding the new parameter, a scaling factor will ease the difficulty of charge emission from negatively charged surfaces which are comparatively easier given if emitting from a positively charged surfaces. Following by this, the future works have now subsequently been using this assumption in their modeling works (Illias et al., 2015). Though, empirical evidence has not been provided in support to these assumptions.

Apart from that, alternative assumptions have been provided to aid the observation of PRPD patterns and this includes incorporating a modified effective work function of the surface, which yields two more free parameters for defining PRPD arrangements based on discharge activity in epoxy resin over a range of applied voltage frequencies.

For this model, a spherical cavity is modelled to observe the PD activity with results tabulated against empirical data. The solution to Poisson's equation was interpreted as a proved field driven by the net electric field in the cavity, which is triggered by surface charge. The initial free electron initiating a PD can segregated into two categories namely, surface emission and volume ionization based on their corresponding equations in association to the derived physical parameters of the material (Dauksys et al., 2016).

Equation CΔUPD was used to compute the real charge magnitude of PD, where UPD represents the voltage drop across cavity when PD is being utilized, which represents the PD's real charge magnitude while the capacitance, C, of the cavity is contingent on the geometry of cavity. The charge induced on the measurement electrode is measurement of apparent charge because of the PD occurrence (Takabayashi et al., 2018). The electrode is reliant on the gas pressure, the location and the shape of cavity, and the cavity's position in relation to the applied field (Jia and Zhu, 2018). Although many studies have shown comparable experimental data and simulation results both quantitatively and qualitatively, there are still some arguments to be found on the of PD's phase and magnitude distributions. Another type of PD model, which utilizes related field improvement evaluation method, is the simulation of streamer PD mechanism at high temperature affected by aging in a spherical cavity enclosed within epoxy resin. All these models can give a good describe on PD event, however, the single value of applied stress is utilized over their experimental work and simulation results (Balamurugan and Venkatesh, 2018).

In brief, Niemeyer's model is proven to be successful in reproducing a range of PD systems in air-filled cavities although inconsistencies are discerned in part of its governing equations where fundamental assumptions made are not clearly justified with high reliance over immeasurable free parameters, which have been adjusted substantially to fit in the experimental data sets (Danikas and Adamidis, 1997).

2.3. Pedersen's model for partial discharge modelling

The induced charge theory model is introduced due to the dispersion of charges on cavity's surface caused by discharges. The discharge process in the cavity is shown in Fig. 4. It is projected that such distributed charges will form an electric dipole composition, which will generate charges on the electrode (Du et al., 2019).

From the figure above, the applied voltage, E0 is parallel and perpendicular to a and b, the dimension of the cavity, while σ represents the charge density across the wall of cavity and q is the induced charge by the cause of dipole composition from PD charges (Lemke, 2016).

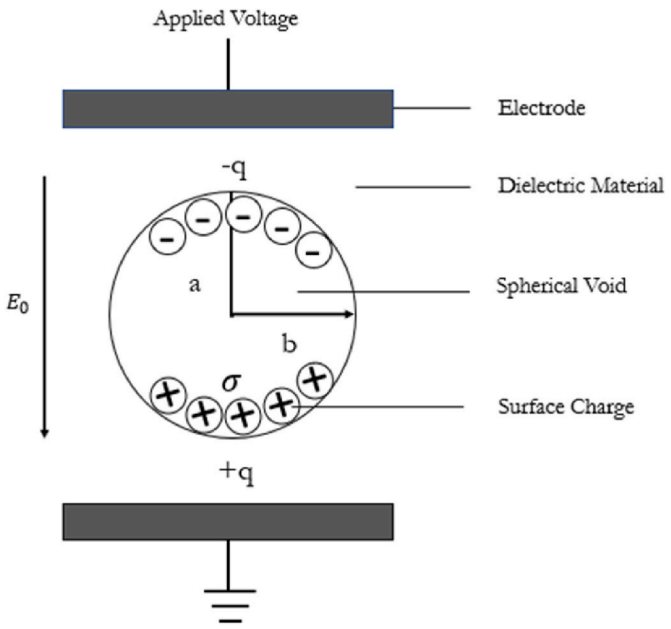

Fig. 4. Discharge process in the cavity.

Pedersen has introduced the concept of induced charge in the year of 1991, which can be employed into partial discharge modelling in a cavity (Arnold and Janicek, 2016). The induced charge can be seen as a change in charge on the electrode before and after the cavity discharge takes place. During PD, charge distribution on the cavity surface raises the surface charge density, which reduces the electric field in the cavity until discharge activity is terminated after a predetermined value is exceeded (Dordizadeh et al., 2015).

The dipole orientation of the positive and negative charges created on both cavity sides is due to the electric field distribution of these charges. The induced charge on the electrode due to charge distribution on the cavity surface is represented by Equation (5) and equation (6) is used to represent the apparent charge magnitude for spherical or ellipsoidal shapes of cavity (Afrouzi et al., 2013).

$$q = -\vec{\mu}\cdot\vec{\nabla}\lambda = -\left(\int_s \vec{r}\sigma dS\right)\cdot\vec{\nabla}\lambda \tag{5}$$

Where the charge deposition on the cavity surface due to the dipole moment induced is denoted by μ in Equation (5). The 'r' is radius vector along the surface whereas 'σ' is the charge density deposited on the surface of the cavity. The dimensionless scalar function is shown by 'λ', which depends solely on the 'ds' position and they can be attained from Laplace's equation.

For the equation above, the induced charge in contact with the electrode or the magnitude of the apparent charge can be expressed in Equation (6), for either the geometry being spherical or ellipsoidal.

$$q = -K\upsilon\varepsilon\,(\mathrm{E_{inc}} - \mathrm{E_{ext}})\mathrm{A}\lambda 0 \tag{6}$$

Besides that, induced charge 'q' also can be defined as Equation (6), the parameter 'K' represents the dimensional constant, which is highly dependent on the cavity's size and geometry and 'υ' is the volume of the cavity. The permittivity of the substantial is represented by 'ε'. In addition, the inception electric field and extinction electric field in the cavity is denoted as $\mathrm{E_{inc}}$ and $\mathrm{E_{ext}}$ individually. E_{inc} is the field at time when PD the occurs whereas the field when PD is halted, is the extinction field and it is represented by $\mathrm{E_{ext}}$, while the solution of the Laplace's equation for the cavity free which is contingent on the location of the cavity, is represented by 'λ0'. Equating λ0 with the value of one at the measuring electrode and λ0 equals to zero at the other electrode, is the

boundary case for solving the Laplace equation (Toader and Mariana, 2000).

The transient response corresponding to the charge induced is seen via discernment of the potential as well as the charge on the electrode prior and post PD (Venger et al., 2017). Prior to the PD taking place, the potential on the electrode as well as the charge remains as V and Q. Upon PD taking place, there will be some noticeable changes in the potential on the electrode, which is decreasing by ΔV, while the charge provided from the outside structure to the electrode is represented by the charge on the electrode increasing by ΔQ. As a consequence, the charge induced on the electrode is recorded with C being the capacitance of the structure (Florkowski et al., 2018). The expression ΔQ in Equation (7) can be ignored, considering the case when the circuit's impedance is sufficient for the current because of discharge.

$$q = C\Delta V + \Delta Q \tag{7}$$

The above method was used in simulating PD occurrences, only taken little time. This model can even be applied in simulating PD inside cavities with cylindrical, ellipsoidal, or spherical shapes in a dielectric material, on the reliance upon a and b parameters as in Fig. 4. The drawback of this model is that they can only be utilized for the case where the field distribution is uniform because the uniformity of the entire cavity is assumed to be afflicted by PD (He et al., 2018). However, this may not apply to cavity of a large size and because of that, the distribution of surface charge across the cavity's wall may not be modelled (Ala et al., 2011).

2.4. Capacitance model for partial discharge modelling

The capacitance model is known as the Whitehead's three-capacitance circuit model or a-b-c model introduced by Whitehead.

Fig. 5 shows the 3-capacitance correspondent circuit that represents the cavity within an insulation material. C_{a1} and C_{a2} in Fig. 5(a) represent the capacitance of the remaining insulator parallel to C_{b1} and C_{b2}. Whereas C_{b1} and C_{b2} replicate the insulator capacitance that is in series with the cavity, C_c in both Fig. 5(a) and (b) is the capacitance's cavity and V is the voltage applied to the circuit. Fig. 5(b) demonstrates the simplified model of three capacitance equivalent circuit. C_a is the correspondent capacitance in parallel of capacitances C_{a1} and C_{a2} while C_b is the correspondent capacitance in series of capacitances C_{b1} and C_{b2} and V_c is the potential crosses the cavity.

In this model, as the inception voltage, U_{inc}, becomes lower than the voltage across cavity V_c, discharge takes place, and diminishes as V_c falls below the extinction voltage, U_{ext}. In the event of discharge's occurrence, C_c will be short circuited which causes a rapid movement of current into the circuit because of the voltage change between C_b and the source. As a result of the immediate voltage depletion by the cause of change in external circuit impedance, a small momentary voltage is generated (Hatiegan et al., 2016).

Before an existence of PD, voltage across cavity (V_c) is equal to

$$V_c = \frac{C_b}{C_b + C_c} V \tag{8}$$

Fig. 5(b) illustrates that, during PD, the magnitudes of the apparent charges (q_{app}) and real charges (q_{real}) are calculated by using equation (9) and equation (10) individually (Afrouzi, 2015).

$$q_{app} = C_b \Delta V \tag{9}$$

$$q_{real} = \left(C_c + \frac{C_a C_b}{C_a + C_b} \right) \Delta V \tag{10}$$

Where Δ V denotes the voltage depletion across the cavity due to discharge. The simplicity and typicality of this model is used to represent the transient happening during an occurrence of discharge, suchlike the apparent charge magnitude and PD current. Nevertheless, the limitation

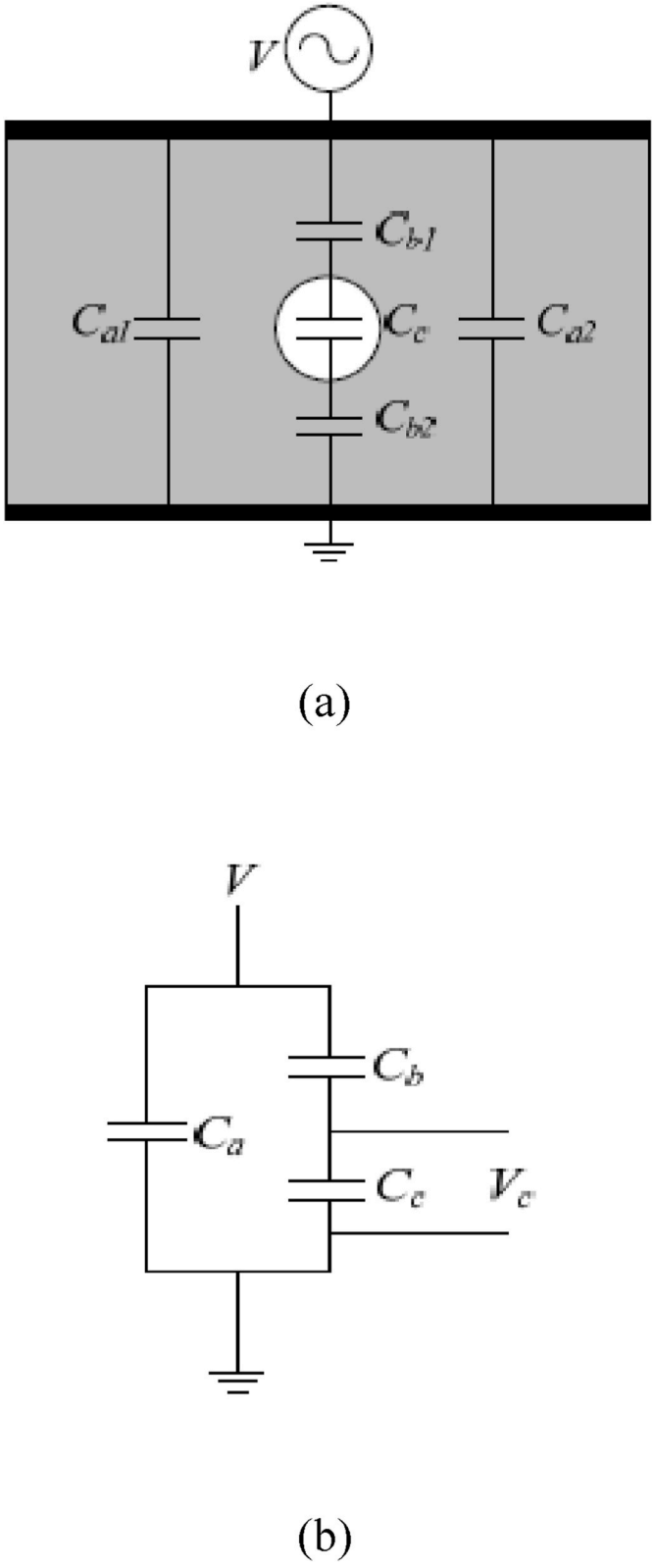

Fig. 5. The equivalent circuit model with three capacitors (a) Full model, (b) Simplified model (Mendiola et al., 2017).

of this model is the surface of the cavity, which is constantly employed as an equipotential surface, which is not often practical for real life application especially with the accumulation of surface charge along the cavity wall being ignored (Achillides et al., 2008).

Overall, this model is suitable in explaining the occurrence of PDs for

academic means as well as a deterministic model. For the a-b-c model to be transformed to a contingent model, the model must be linked with an analytical approach. Research by Callender et al. (2019) described a hybrid model that integrates the three-capacitance correspondent circuit model with Pedersen's doctrine by means of a time variable conductance. Additionally, the traditional detailed model is one of the models utilized in PD research. The low frequency validity range of the traditional detailed model, which is confined to around 1 MHz is one of the underlying issues. Resultingly, the transient state behavior of transformer winding was investigated by Baravati et al. (2022) using an improved detailed model that included stray capacitance in addition to the traditional detailed model.

To determine the winding's reaction to the application of the PD signal, a general state-space technique was proposed. Which determines the winding response corresponding to the application of PD between two sections and between winding sections and the ground by evaluating two distinct state-spaces. The revised detailed model's frequency dependent parameters were derived using the finite element approach (FEM). Additionally, new approaches and ideas were implemented and evaluated on an actual 20 kV distribution transformer winding as well as a 63/20 kV, 30 MVA winding. The accuracy and wider frequency validity range of their proposed model was shown by comparing the waveforms recorded in the laboratory utilizing PD pulses on both windings.

In addition, the effect of lower order supraharmonics on partial discharge activity in an insulation system sample with a predetermined spherical cavity defect was examined by Sefl and Prochazka (2022). The supraharmonics were represented by sinusoidal oscillations with a shape, amplitude, and natural frequency based on typical trends detected or estimated in medium to high voltage electric sub grids with power converters. The test sample was subjected to a combination of a fundamental 50 Hz waveform and a one-per-period oscillation, and the resulting partial discharge activity was monitored.

Moreover, the position and natural frequency of the oscillation were gradually modified throughout the experiment. After that an analytical model was used to replicate partial discharge activity under identical conditions, and the phenomena seen during the experiment were described by it. The model has been updated to account for the presence of supraharmonics oscillators. Finally, inferences were reached about the significance of variations in partial discharge activity. Predictions of a higher ageing rate, an earlier start to partial discharge activity and continued research as a future work were among them.

This model aids in the illustration of a dielectric material's isolated cavity (Pan et al., 2011). The instantaneous variation in the capacitance charging process of the test object is the characteristic of this particular partial discharge model (Callender et al., 2017). Although this capacitance circuit is simple and deterministic, its statistical behavior is full of complexity which is not applicable for cavity properties description in actual circumstance as in reality, the surface of the cavity is not equipotential and surface charge tends to gather on the exterior of cavity after a discharge occurs. Despite that, an improved version of 'abc' model has also been introduced. This improved model employed the consideration of the accretion of charge on the surface of cavity upon PD occurrence. The discharge has been calculated as a voltage and time dependent resistance, which encapsulates the discharge progression, that is a change in the cavity from insulation to conduction (Callender et al., 2018).

2.5. Plasma PD models

The gas discharge procedure in Plasma PD models is simulated using the fluid equations. These equations describe the ionization impact, drift of charge, diffusion, recombination, and other secondary effects (Xu et al., 2017). This model has successfully attained the evolution of electric field as well as the distribution of the absorption of charge inside the cavity due to the discharge procedure and the discharge current pulse (Mor and Heredia, 2018). In plasma model, physical discharge processes had been reflected tremendously with large amount of data attained to obtain the repetitive PD pulses and their stochastic parameters because of stochastic nature (Joseph et al., 2019).

However, there is an inclination of considering excessive substantial discharge process which increases model complexity and add up large calculation work to be done which diverse the results for statistical analysis (Wang et al., 2017). As a result, only selected, and important processes such as the streamer development and surface process will be considered in this simulation model (Achillides et al., 2017). The pulse current technique which detects the apparent charge are governed by the streamer growth within the cavity while the surface procedure consists primarily of the charge accretion on the interface and the radiation of charge at the surface (Kim et al., 2004). For the subsequent PD to be provided with free electrons it relates to the process known as surface emission. This process describes that when a streamer lands on the surface of dielectric, charge will accumulate which subsequently affect the behavior of PD (Dordizadeh et al., 2016). In this model, it is noted that surface charges fluctuate through the subsequent one after previous discharge. Accumulated charges decay as a result of surface or bulk conductivity of dielectric (Romano et al., 2018). In brief, a single PD process is represented by the streamer growth as well as surface charge accretion. In addition, during a partial discharge series, the interconnection of adjacent discharges is represented by the surface charge accretion, decomposition, and radiation, which should be examined in this simulation model (Yousfi and Lefkaier, 2018).

This model has presented a rigorous approach, which is to use the drift diffusion formulas for 3 charged categories, specifically an electrostatic equation in verifying the electric field and 3 Helmholtz equations to find out the photoionization rate (Liu et al., 2018). Besides, this simple drift diffusion model does consider the electrons and virtually positive and negative ions, which aids in analyzing the phenomena of PD (Calcara et al., 2017). This model will then solve the drift diffusion equations for the number densities of electrons ne, positive ions np and neutral ions nn, as shown below (Driessen et al., 2019).

$$\frac{\partial n_e}{\partial t} = \alpha n_e \left|\overrightarrow{W_e}\right| - \eta n_e \left|\overrightarrow{W_e}\right| - \beta n_e n_p - \overrightarrow{\nabla}.\overrightarrow{\Gamma}_e + S_{ph} \tag{11}$$

$$\frac{\partial n_p}{\partial t} = \alpha n_e \left|\overrightarrow{W_e}\right| - \beta n_n n_p - \beta n_e n_p - \overrightarrow{\nabla}.\overrightarrow{\Gamma}_p + S_{ph} \tag{12}$$

$$\frac{\partial n_n}{\partial t} = \eta n_e \left|\overrightarrow{W_e}\right| - \beta n_n n_p - \overrightarrow{\nabla}.\overrightarrow{\Gamma}_n, \tag{13}$$

Where N is the charge number density, e, p and n are the symbols for electron, positive ion and negative ion, β and D_e denote the recombination and electron diffusion coefficients. Drift velocity, W is denoted as the production of electric field and charge mobility whereas S_{sec} indicates the source term about secondary process eg. Photoionization and cathode secondary emission.

A thorough plasma dynamics of the discharge along with motion of electrons, and ions will be exhibited. A lot of simulations are done on this model, typically on modelling discharges from a needle-plane electrode configuration without solid dielectric materials present while investigating barrier of dielectric discharges (Kim and Siada, 2018). The simulations conducted are found to have restricted vision inside PD event for systems as they are normally carried out for system of interest such as sterilization, or material processing at the range of power frequencies of 50–60 Hz under significantly different physical conditions from the standardized PD systems (Singh et al., 2018).

The drift diffusion equations were employed in the modelling of an extensive figure of partial discharge in an air gap confined by two electrodes, one on top and the other are covered with the insulation dielectric material (Ahmed and Srinivas, 1998).

The modelling work of plasma diffusion model focuses on air filled spherical cavity, specifically on spherical cavity bounded by epoxy resin

has been a general research subject over these recent years (Renforth et al., 2019). The attained results had been scrutinized in qualitative method in parallel to the experimental results obtained to enhance the understanding of the physics behind PD event. Not all parts of the research on PD using this modelling technique have been done perspicuously (Danikas et al., 1991). However, PD activities occurring within the spherical cavities with surrounding liquid insulation is considered a similar system with the same physical means of gaseous cavity inside the homogeneous dielectric material, which have been proven and examined by a few simulations works (Cavallini and Montanari, 2006). The outcome based on these simulation works ascertained the statement whereby when cavities in either liquid dielectric or solid dielectric are confined by the akin physical conditions, the discharges within the system are seen to include an electron avalanche that has been transformed into a positive streamer, which is consistent with the principle of dielectric barrier discharges.

The undercurrents of plasma model are approximately discrete owing to the discharge enclosed within the cavity, which refrain the plasma from spreading. Moreover, previous research has emphasized the initialization of PD as well as plasma dynamics. The objectives of this model are to enhance the insight of undercurrents of partial discharge as well as to experiment the previously employed PD concepts in past modelling of discharge activities in gaseous voids.

In the concept of plasma model, plasma dynamics of PD in gaseous cavity has been defined as an electron avalanche that transforms into a positive streamer in favor of a dielectric barrier discharge occurring in a 3 mm air gap with an attained electric field that is slightly higher than the breakdown brink of the air. The simulations study conducted on cavities in liquid dielectric has testified the concept of plasma model, discerning as the indicative of PD systems in spherical cavities. The overall results have revealed that the conception of plasma dynamics where the motion an electron avalanche in oppose to the applied electric field revolute into a positive streamer travelling in parallel to the electric field (Forssen and Edin, 2008).

In partial discharge modelling, the two fundamentals and prevalent values employed are the inception and residual fields. This is because the occurrence of PD activity is often triggered by some critical value of electric inception or inception field (E_{inc}) archetypically at the very center of the cavity. The E_{inc} for a standardized PD system is expressed as the equation below:

$$E_{inc} = \left(\frac{E}{p}\right)_{cr} P\left(1 + \frac{B}{(pl)^{1/2}}\right) \tag{14}$$

where $\left(\frac{E}{p}\right)_{cr}$ has a value of 25.2 V Pa-1 m-1. It is known as the proportionality constant between the critical electric field E_{cr} needed in sustaining discharge and the gas pressure p, with B = 8.6 Pa1/2 m1/2. The value of 'l' in the equation will represent the length of the cavity in the discharge direction. The point to be taken note in the employment of this equation is that the constant, $\left(\frac{E}{p}\right)_{cr}$ is contingent on the polarity of on streamer. It is only then being deduced that the electric field in the cavity has decreased to a residual value, which is equivalent to the electric field in the streamer channel, Ech right after the discharge has occurred. The value of electric field in streamer channel, E_{ch}, will be proportional to E_{cr}. The relation between the electric field in streamer channel (E_{ch}) and critical Field (E_{cr}) shown by equation 15

$$E_{res} = E_{ch} = \gamma E_{cr} \tag{15}$$

where γ has a value of 0.35, with a positive streamer average value of 0:2 and a negative streamer average value of 0:5. Although these equations have been prevalently used in past literature, typically being proposed in the cited work of Niemeyer, the applications of these equations in PD systems are still raising skepticism. This is because the methods used in determining of inception equations for the experimental and modelled PD systems are entirely different (Arnold and Janicek, 2016). In experimental work, the inception equation is resolved based on the ionization parameters revolving around the electrical disintegration in air gaps between metallic electrodes, whereas in partial discharge structures, the creation of the electric field inception equations originated from the PD region surrounded by solid dielectric material (Schifani et al., 2001).

Moreover, there is uncertainty relative to the residual electric field equation whereby there is some possibility being overlooked whereby the electric field in the streamer channel might no longer be equal to the field, E_{cr} after discharge event has died down. Apart from that, the inference established, deducing that the streamer channel field is relational to the critical electric field is in fact, depicted from metallic needle-plane experiments, which diversifies from the original PD systems and standardized physical conditions with homogenous applied field, and bounded solid dielectric regions. So, the employment of these equations is highly restraint to only certain type PD systems.

The surface charge distributions in plasma model are deduced to be bipolar at times when there are symmetrical dielectric surfaces in either spherical, cylindrical, or ellipsoidal cavities at each side of a discharge channel. However, early experiment and numerical analysis conducted on PD investigation in cylindrical cavities has inferred that the surface charge distributions of PD systems are not bipolar (Schifani et al., 2001). This is because there is a greater spread of negative surface charge distribution than the positive surface charge distribution due to higher kinesis in electrons as compared to ions. Both studies are governed at that instantaneous period right after the electric fields has surpassed its breakdown threshold for initializing PD.

Previous modelling work of PD has deduced the surface charge of former PD will directly be buried due to the deposition of surface charge of the new PD (Pan et al., 2016a). Still, there is still a possibility that the electric field induced by the surface charge of earlier PDs will affect the charge adopted by the following PDs.

Besides, the process of charge recombination is governed by the plasma model where in Niemeyer paper, an order of the time delays constant magnitude, τ_{rec}, was computed to obtain the charge recombination rate within a cavity upon a discharge occurrence as below.

$$\tau_{rec} \sim \frac{l}{C_{\mu}\left(\frac{E}{p}\right)_{cr}} \frac{E_0}{E_{inc}} \tag{16}$$

where l is the cavity's length scale, C_{μ} is the proportion of ion mobility affected by gas pressure, p is the gas pressure and E_0 is the magnitude of electric field applied (Danikas et al., 1991). Most PD systems are governed in the order of microseconds and because of that the effect of leftover charge by the earlier PDs is negligible as the time delay is very short whereby time for the next discharge occurs is going to be the subsequent order of milliseconds (Pedersen et al., 1993).

Although the numerical analysis methods utilized in this task comes to reducing the computational cost, the minor details and parameters change in the model system could eventually influence the overall results and that the procedures must be done with extra caution (Liu et al., 2017). Despite a recent improved model of the same type was successfully applied in designing various discharges in a spherical void cavity, it is indisputably that the results relating PD using this method are still imperfect with speculative high level of asymmetry of the model solved in a 3D geometry. Nevertheless, this model marks an advance step into developing numerical analysis techniques in resolving the major equations revolving partial discharge through axisymmetric physics and geometry (Cavallini and Montanari, 2006).

The fallback of this model is that the behaviors of continuous PDs cannot be represented owing to the storing fallout. A change in the next PD characters occur as a result of the continuing charges produced by the former PD landing on the surface of the cavity which subsequently

influence the electric field dispersion inside the cavity. A partial discharge simulation should include investigation of the physical parameters as well as multiple data to obtain the statistical parameters of repetitive PDs, due to their statistical characteristics. It is concluded that plasma model provides in-depth understanding of the physical parameters of the partial discharge for a single PD only. Ergo, a simulation model which represent the discharge growth procedure while considering the memory effect should be established to attain the stochastic characters of PD sequences.

2.6. Summary

An overview of PD as well as a description of the existing literature on PD modelling is provided in this section. Although many of the concepts may be tracked back to Niemeyer's pioneering work as a variety of PD models have been developed. For a number of studies, such as cylindrical or spherical air-filled gaps enclosed by a solid dielectric substance such as polyethylene or epoxy resin PD models have proved successful in recreating PRPD patterns. A Poisson PD model is recommended above Niemeyer's model, ABC model, Pedersen model, and plasma model according to the literature review. Because it enables full resolution of the defect geometry, knowledge of the electric field and explicit calculation of the apparent charge at all points in the PD system.

Many PD models have been developed in the past with an aim to overcome flaws of prior FEA Poisson model, particularly their reliance on many free parameters. Many previous models contained a large number of free parameters, which is said to provide a more physical explanation of the PD process and allow the model results to suit experimental data.

3. Charge decay by conduction along the surface in different models

Accretion of charges on the cavity wall occurs upon a discharge moving freely across the whole cavity wall or being trapped on the cavity surface. In charge decay, free charges are generally being assumed to travel via conduction of the surface on cavity wall. Moreover, the motion of such charges is highly contingent on the magnitude and direction of cavity field $E_{cav}(t)$ and field from the surface charge $E_s(t)$ (Alsheikhly et al., 1992). Apart from that, it is deduced that the motion of surface charges is towards the symmetrical axis with the direction of $E_{cav}(t)$ distinctive from $E_s(t)$. Due to this case, there arises the limitation of charge movement on the wall's cavity. On the other hand, recombination of charge is caused, when $E_{cav}(t)$ is in the same direction as $E_s(t)$, the free charges on the cavity wall are inferred to be moving away from their deposited location while approaching the charges with the opposite polarity. The number of charges deposited on the surface then decrease; causing $E_s(t)$ to reduce. The rate of free charges on the surface moving across the cavity surface is highly reliant on the electrical conductivity of cavity surface, σ_s. The higher the σ_s, the faster the motion on charge induced.

The conduction of charge on the wall's cavity is represented differently by each partial discharge model. However, in the a-b-c equivalent capacitance model, charge conduction is not modelled as a result of free charges on the surface accumulated being unavailable. As for Niemeyer's model, the degradation of the surface charge Δq_s in contact with the cavity wall is predicted adopting Ohm's law while obtained using equation (17) (Cavallini and Montanari, 2006).

$$\Delta q_s = -\left(\pi/2\right) 2aE_{cav}\,\sigma_s \Delta t \tag{17}$$

Where the instantaneous voltage drop across the cavity wall is represented by $2aE_{cav}$, the cavity field is defined as E_{cav}, σ_s is the electrical conductivity of cavity surface while $\pi/2$ is the geometrical factor and Δt is the stepping time interval.

In electric current FEA model (Fig. 2), the conductivity of cavity surface, σ_s is being raised to a greater value to design the charge motion by surface conduction across the cavity surface (Chen and Baharudin, 2008). While in electrostatic FEA model, the surface charge reduction on each of the cavity surface region (Fig. 3) is computed using equation in (Pan et al., 2016b).

4. Discussion and comparison between partial discharge models

Based on a critical review of the existing PD models, the following conclusions can be drawn (Time, cost, Degree of application). Based on Table 1, the advantages of using the Finite Element model outshines the others model as it allows the modelling of the PD system of interest to be easily achieved through computing the electric field strength and direct evaluation of real and apparent charges due to the approximations of PD system geometry (Cavallini and Montanari, 2006). However, one disadvantage that comes along with this technique is that many parameters will be needed for curve fitting.

In contrary, although Pedersen's model can provide precise numerical correlation between measured transient and induced charge, this model is unsupported by employment of theoretical approaches whereby the complexity of the computation will be increased (Dordizadeh et al., 2016).

$$\Delta q_S = -\sigma_S \Delta t \int_S E_{Si}\mathrm{d}S \tag{18}$$

Equation (18) is used to calculate the amount of surface charge, where Est is the tangential field along the cavity wall of surface element, dS. Δq_S is deducted from the cavity surface region and subsequently being joined to the contiguous surface region, conditional on the direction of charge motion on the cavity wall. Δq_S is increased to the subsequent area which is nearer to the axis of symmetry if the charge moves to the symmetrical axis, else it will be joined to the area farther from the symmetrical axis. As a consequence, the recombination of charge in the event of meeting of charges from the lowermost and uppermost cavity surfaces causes a decrease in the number of surface charge.

The speed of charge movement from one area to another area is affected by the number of surface areas where charge propagates in the event of a discharge. As a result, the electrical conductivity of cavity surface for the simulation may vary, contingent on the prediction deduced on the motion of charge across the cavity wall. Based on Fig. 3, the simulation of epoxy resin covers a justifiable surface conductivity when the surface region was being divided into 10 identical regions.

Although the simulations showed that the time step interval has no compelling impact on the cavity field alteration, the number of charges disintegrating with time may vary as smaller stepping time leads to a more rapid decline in the number of surface charge. In brief, as various time step used, no significant alteration occurs to the charge dispersion on the cavity surface. Consequently, the electric field dispersion inside the cavity surface independence as of the simulation time step used.

With reference to the simulation work by Illias et al. (2011a), different simulation parameter values are used for different PD model where (S1- Niemeyer model, S2 – Electric current FEA model & S3 – Electrostatic FEA model). Material and cavity conductivities are only designated for electric current FEA model (S2) as current is deduced to

Table 1
Summary of the mechanism of charge conduction on the cavity surface for each Pd model (Illias et al., 2011a).

PD Model	Decay charge modelled via surface conduction
Three-Capacitance Model	–
Niemeyer model	$\Delta q_s = -\pi\alpha E_{cav}\sigma_s \Delta t$
Electric Current FEA Model	The cavity surface conductivity is being increased
Electrostatic FEA Model	$\Delta q_s = -\sigma_s \Delta t \int_S E_{st} dS$

move in the substantial as well as the cavity while the initial surface charge density ρ_{s0} is set for the electrostatic FEA model, which is used to increase the density of charge along the cavity wall during PD occurrence. While the parameters such as the inception field, N_{es}, N_{ev} and charge decay time constant remain the same for these models.

However, different electrical conductivity of the cavity surface, σ_S for movement of charges along the cavity surface and extinction field, E_{ext} are acquired for various PD models. This is the result of different approaches that are used in calculating the electric field of the cavity and PD apparent charge magnitudes. This may be noted for the case where the maximum field in the cavity without PD occurs, E_{cavma} is different for each model while the extinction field, E_{ext} is determined by the minimum PD charge from the measurement since PD charge is highly dependent on the cavity field reduction after PD occurrence. As a result, different ways to calculating charge magnitude provide diverse relationships between cavity field change and charge magnitude.

The cavity surface conductivity, σ_s is derived through comparison between the optimum PD charge on the charge magnitude phase axes between $\varphi - q - n$ plots of the simulation and measurement (Illias et al. (2011b). The reasonable value of the cavity surface conductivity for each model is $10^{-14} to 10^{-7} Sm^{-1}$. In Niemeyer 's model, the movement of charge via surface conduction is evaluated using equation (19) while for electrostatic FEA model, surface charge conduction is highly dependent on the regions that cavity surface is being divided. The more regions that surface is being divided, the slower E_s decreases. This is as a result of slower disintegration ratio number of surface charge for 10 surface regions since more stepping time interval is needed to shift from a surface region to the encounter point of the lowermost and uppermost cavity surfaces where charge recombination takes place.

The electric current as well as the electrostatic FEA models can simulate the decay rate of the surface charge electric field $E_s(t)$ using different cavity surface conductivity, σ_s. Under high electric field stress, the electric field distribution of the cavity alters after discharge occurrence due to the motion of charge on the cavity wall. In both FEA models, higher σ_s will induce greater charge motion on the surface of cavity, leading to higher rate of surface charge deduction due to recombination of charge and faster depletion rate of. $E_s(t)$.

In brief, all the PD models show that the magnitude of charge increase with the diameter of cavity which are validated by the experimental work on cavity dielectric material (Madhar et al., 2021). The size of the cavity decides the optimum propagation length of an electron avalanche which goes in equal direction as the applied voltage while the avalanche goes perpendicular with the applied voltage. The greater the electron avalanche propagation length in larger cavity size will result in higher charge magnitude.

For capacitance model, it offers a few advantages such as allowing direct association between space charges and variation of capacitance with number of space charges within the cavities of insulator evaluated but the major downfall of this model is the incapability of replicating the mechanism of PD within gaseous cavities surrounded by solid dielectric (Chen and Baharudin, 2008). Apart from that, the reason that they are having a low degree of application is because the concept highly opposes the real-life specifications where there is a misrepresentation between apparent charge with induced charge (Daphne et al., 2019b).

A comparison of different partial discharge modelling techniques is given in Table 2. Moreover, advantages and limitations of each model is summarized in Table 3.

Table 2
Comparison between different partial discharge modelling techniques.

PD Models	Finite Element	Pedersen's	Capacitance	Plasma	Niemeyer
Time	Lengthy	Average	Short	Average	Average
Cost	Average	High	Low	Low	Average
Degree of Application	Easy & Accurate	Average	Low	Low	Low

Plasma PD Model is considered a newly developed model, which signifies the introduction of numerical analysis techniques in solving PD activities. However, this model is only applicable to limited systems such as material processing and sterilization. In brief, they are still imperfect with speculative high level of asymmetry of the model solved in a 3D geometry (Riande and Calleja, 2013). On the other hand, Niemeyer's model provides flexibility by introducing free parameters in assisting the investigation of PRPD patterns for spherical cavities in the insulation system under varying physical conditions. Withal, they are not applicable to all PD systems of interest since they are having limited employability to only spherical gaseous cavity bounded by epoxy and an

Table 3
Advantages and Limitations of PD models.

PD Models	Advantages	Limitations
FEM	• Pre-discharge event is learnt by obtaining field interruption figures. • Accurate model by measuring the apparent charge magnitude by time integration of current • Possible to model using 3D geometry and significant analysis in term of boundary setting	• Large amount of data is required for the meshing process • It requires a digital computer and fairly extensive
Niemeyer's Model	• The fundamental for most of the PD modelling. • Propose the mathematical model consider of initial electron generation, model of streamer process and the estimation of PD charge magnitude. • Propose equation of cavity surface emission and volume ionization.	• Not accurate due to fundamental assumptions made • Fundamental assumptions made are not clearly justified with high reliance over immeasurable free parameters. • Some parameters assume to be constant such as cavity surface charge. • The induced charge assumes that the void internal field remains constant, and the entire section of the void undergoes the discharge procedure.
Pedersen's Model	• Introduced the induced charge concept which is associated with partial discharge in a cavity • Propose the model of induced charge theory and consider the induced charge on the electrode before and after a discharge occurrence in the cavity. • This type of models distinguishes the PD occurrence from the perspective of field model	• It can only be used when field distribution is uniform because the uniformity of the entire cavity is assumed to be afflicted by PD. However, this may not apply to cavity of a large size and due to that, the distribution of surface charge across the cavity's wall may not be modelled • The induced charge assumes that the void internal field remains constant, and the entire section of the void undergoes the discharge procedure
Capacitance Model	• The capacitance models are concise • An easy model to apply to power equipment such as power cables • The model is used to simulate multiple PDs.	• When the cavity surface is equipotential then void capacitance can be used. • Distribution of surface charges causes non-uniformity, leading the cavity surface being equipotential after a PD.
Plasma Model	• The mode presents in-depth details and physical understanding into the discharge phenomenon for a single PD	• Simulating multiple PDs are difficult as complex physical activities lead to difficulty in modeling the PD as well as huge methods of computation.

electrode protrusion in SF6 with inconsistent governing equations and ambiguous fundamental assumptions (Danikas et al., 1991). This model also requires an exact scaling factor to precisely replicate the typical rabbit ear discharge, which adds up the workloads of researchers and with high dependency over immeasurable free parameters, the researchers deploying this technique will again being forced to adjust the free parameters significantly to fit in different sets of experimental data.

5. Conclusion

An overview to PD has been provided in this article along with a summary of different PD modelling techniques to enhance the comprehension of partial discharge dynamics. Although an assortment of PD models has been developed, the foundational concepts of these developed PD models are all established based on Niemeyer's model. The resultant PRPD patterns had been successfully generated during the experiments of different PD models, in customary the cylindrical or spherical air-filled cavities in a solid dielectric insulation, which comprises of either polyethylene or epoxy resin. Despite that, a few limitations and inconsistencies have been discerned in many of these PD models. Among all these PD models developed, Poisson PD model that is resolved using FEA is chosen over Niemeyer's model, ABC model, Pedersen model and Plasma model as the defect geometry can be resolved completely with calculation of apparent charge done explicitly and thorough phenomena of electric field at all locations in PD system provided. Apart from that, since the quick process of gas recombination, where changes in the surface charge density at the surface of cavities can be detected, the Poisson model has proven to be more physically accurate. However, the dependence on high figure of free parameters is found to be the shortcomings of previous FEA Poisson models, although it is argued that using high figure of free parameters are going to fit the model results to experimental data. A problem which occurs with this method is that the model gradually becomes a curve fitting application and loses physical applicability. Even though it is impossible to eliminate free parameters due to the limited data available from the PD system, work should be done to reduce the number of free parameters. It may be prominent that as the characterization of the procedure of discharge remains a significant simplification in this model, and it might be impossible to discard numerous drawbacks related with former PD models. Throughout the research, it became evident that the drawbacks of modified PD model are still considerable. Particularly, it is unclear whether majority of the theories used in the model are justified. This research schemes the essential contribution, which significantly reconsiders the necessity of PD modelling, exclusively if the more complicated PD systems existing in the field are to be considered.

Credit author statement

Hadi Nabipour Afrouzi: Supervision, preparing the first draft., **Ateeb Hassan**: Reviewing and Editing.**Daphne Tay Ye Chee**: Revising the first draft, Editing., **Kamyar Mehranzamir**: Validation, Reviewing and Editing, **Zulkurnain Abdul Malek:** Supervision, Validation, and Reviewing., **Saeed Vahabi Mashak:** Validation, Reviewing and Editing and **Jubaer Ahmed:** Reviewing and Editing.

Authors' contributions

All the authors had participated in preparing the manuscript.

Declaration of competing interest

The authors declare that there is no conflict of interest.

References

Achillides, Z., Danikas, M.G., Kyriakides, E., 2017. Partial discharge modeling and induced charge concept: comments and criticism of pedersen's model and associated measured transients. IEEE Trans. Dielectr. Electr. Insul. 24 (2), 1118–1122. https://doi.org/10.1109/TDEI.2017.006013.

Achillides, Z., Georghiou, G.E., Kyriakides, E., 2008. Partial discharges and associated transients: the induced charge concept versus capacitive modeling. Dielectr. Electr. Insul. IEEE Trans. 2008 15 (6), 1507–1516. https://doi.org/10.1109/TDEI.2008.4712652.

Adam, B., Tenbohlen, S., 2021. Classification of superimposed partial discharge patterns. Energies 14 (8), 2144. https://doi.org/10.3390/en14082144.

Afrouzi, H.N., 2015. Characterisation of Partial Discharge Phenomenon in High Voltage Insulation Using Finite Element Method and Matlab Simulink. PhD Dissertation. Universiti Teknologi Malaysia.

Afrouzi, H.N., Malek, Z.A., Mashak, S.V., Naderipour, A.R., 2013. Three-dimensional potential and electric field distributions in HV cable insulation containing multiple cavities. Adv. Mater. Res. 845, 372–377. https://doi.org/10.4028/www.scientific.net/AMR.845.372.

Ahmed, N., Srinivas, N., 1998. On-line partial discharge detection in cables. IEEE Trans. Dielectr. Electr. Insul. 5 (2), 181–188. https://doi.org/10.1109/94.671927.

Ala, G., Candela, R., Romano, P., Viola, F., 2011. Simplified hybrid PD model in voids. In: IEEE International Symposium on Diagnostics for Electric Machines, Power Electronics and Drives, Bologna, Italy, September 5-8, pp. 451–455. https://doi.org/10.1109/DEMPED.2011.6063662.

Ali, N.H.N., Rapisarda, P., Lewin, P.L., 2018. Multiple partial discharge signal decomposition using mathematical morphology. In: 2018 IEEE Conference on Electrical Insulation and Dielectric Phenomena (CEIDP), Cancun, pp. 514–517. https://doi.org/10.1109/CEIDP.2018.8544902.

Alsheikhly, A., Guzman, H., Kranz, H.G., 1992. A new diagnostic tool through computer simulation calculation using expanded partial discharge equivalent circuit. In: 1992 Proceedings of the 4th International Conference on Conduction and Breakdown in Solid Dielectrics, 176 – 180. https://doi.org/10.1109/ICSD.1992.224982.

Alsheikhly, A., Kranz, H.G., 1991. A new approach for a basic understanding of PD-phenomena. In: 7th International Symposium on High Voltage Engineering, pp. 25–28.

Arnold, P., Janicek, F., 2016. Modelling of Partial Discharge Activity, 2016 Diagnostic of Electrical Machines and Insulating Systems in Electrical Engineering (DEMISEE), Papradno, pp. 34–37. https://doi.org/10.1109/DEMISEE.2016.7530482.

Aziz, N.H., Catterson, V.M., Rowland, S.M., Bahadoorsingh, S., 2017. Analysis of partial discharge features as prognostic indicators of electrical treeing. IEEE Trans. Dielectr. Electr. Insul. 24 (1), 129–136. https://doi.org/10.1109/TDEI.2016.005957.

Balamurugan, H., Venkatesh, S., 2018. A review on deterministic and stochastic models for electrical treeing initiation and propagation in solid insulation systems from the perspective of prediction assessment techniques. Int. J. Eng. Technol. 7 (4), 2271–2290.

Baravati, P.R., Moazzami, M., Hosseini, S.M.H., Mirzaei, H.R., Fani, B., 2022. Achieving the exact equivalent circuit of a large-scale transformer winding using an improved detailed model for partial discharge study. Int. J. Electr. Power Energy Syst. 134, 107451 https://doi.org/10.1016/j.ijepes.2021.107451.

Calcara, L., Pompili, M., Muzi, F., 2017. Standard evolution of Partial Discharge detection in dielectric liquids. IEEE Trans. Dielectr. Electr. Insul. 24 (1), 2–6. https://doi.org/10.1109/TDEI.2016.006499.

Callender, G., Lewin, P.L., Montanari, G.C., 2018. Simulation of partial discharge under impulse voltage waveforms. In: 2018 IEEE 2nd International Conference on Dielectrics (ICD), pp. 1–4. https://doi.org/10.1109/ICD.2018.8514585.

Callender, G., Rapisarda, P., Lewin, P.L., 2017. Improving models of partial discharge activity using simulation. In: 2017 IEEE Electrical Insulation Conference (EIC), pp. 392–395. https://doi.org/10.1109/EIC.2017.8004653.

Callender, G., Tanmaneeprasert, T., Lewin, P., 2019. Simulating partial discharge activity in a cylindrical void using a model of plasma dynamics. J. Phys. Appl. Phys. 52 (16), 055206 https://doi.org/10.1088/1361-6463/ab0194.

Castro, B., Clerice, G., Ramos, C., Andreoli, A., Baptista, F., Campos, F., Ulson, J., 2016. Partial discharge monitoring in power transformers using low-cost piezoelectric sensors. Sensors 16 (8), 1266. https://doi.org/10.3390/s16081266, 2016.

Cavallini, A., Montanari, G.C., 2006. Effect of supply voltage frequency on testing of insulation system. IEEE Trans. Dielectr. Electr. Insul. 13 (1), 111–121. https://doi.org/10.1109/TDEI.2006.1593409.

Chalaki, M.R., Yousefpour, K., Klüss, J., Kurum, M., Donohoe, J.P., Park, C., 2021. Classification and comparison of AC and DC partial discharges by pulse waveform analysis. Int. J. Electr. Power Energy Syst. 125, 106518 https://doi.org/10.1016/j.ijepes.2020.106518.

Chen, G., Baharudin, F., 2008. Partial discharge modelling based on a cylindrical model in solid dielectrics. Int'l. Conf. Condition Monitor. Diagn. 74–78. https://doi.org/10.1109/CMD.2008.4580233.

Crichton, G.C., Karlsson, P.W., Pedersen, A., 1989. Partial discharges in ellipsoidal and spheroidal voids. IEEE Trans. Electr. Insul. 24 (2), 335–342. https://doi.org/10.1109/14.90292.

Danikas, M., Adamidis, G., 1997. Partial discharges in epoxy resin voids and the interpretational possibilities and limitations of Pedersen's model. Electr. Eng. 80 (2), 105–110. https://doi.org/10.1007/BF01245959.

Danikas, M., McAllister, I.W., Crichton, G.C., Pedersen, A., 1991. Discussion: partial discharges in ellipsoidal and spheroidal voids. IEEE Trans. Electr. Insul. 26 (3), 537–539. https://doi.org/10.1109/14.85127.

Daphne, T.Y.C., Afrouzi, H.N., Abdul-Malek, Z., Kamyar, M., Jubaer, A., 2019a. Study of electric field distribution in the high voltage stator bar insulation in presence of

different shapes, locations and sizes of cavities. AIP Conf. Proc. 2173 (1), 020012 https://doi.org/10.1063/1.5133927.
Daphne, T.Y.C., Afrouzi, H.N., Abdul-Malek, Z., Kamyar, M., Jubaer, A., Tiong, S.K., 2019b. Simulation and analysis of electric field distributions in stator bar insulation system with different arrangement of cavities. IEEE, Int. UNIMAS STEM 12th Eng. Confer. (EnCon) 4 (3), 87–91. https://doi.org/10.1109/EnCon.2019.8861258.
Dauksys, G., Jonaitis, A., Gudzius, S., Morkvenas, A., 2016. Investigation of partial discharges at the high voltage electric motor bars, Elektron. ir Elektrotechnika 22 (2), 9–12. https://doi.org/10.5755/j01.eie.22.2.6983.
Dordizadeh, P., Adamiak, K., Castle, G.S.P., 2015. Numerical investigation of the formation of trichel pulses in a needle-plane geometry. J. Phys. Appl. Phys. 48 (41), 415203 https://doi.org/10.1088/0022-3727/48/41/415203.
Dordizadeh, P., Adamiak, K., Castle, G.S.P., 2016. Study of the impact of photoionization on negative and positive needle-plane corona discharge in atmospheric air. Plasma Sources Sci. Technol. 25 (6), 065009 https://doi.org/10.1088/0963-0252/25/6/065009.
Driessen, A.B.J.M., Duivenbode, J.V., Wouters, P.A.A.F., 2019. Operational conditions influencing the partial discharge performance of cables under low and medium vacuum. IEEE Trans. Dielectr. Electr. Insul. 26 (1), 81–89. https://doi.org/10.1109/TDEI.2018.007536.
Du, Y., Meng, Y., Wu, K., Yang, X., Wang, Y., 2019. Influence of gas flow on partial discharge behaviors in air and nitrogen. IEEE Trans. Plasma Sci. 47 (1), 136–144. https://doi.org/10.1109/TPS.2018.2879218.
Florkowski, M., Florkowska, B., Kuniewski, M., Zydron, P., 2018. Mapping of discharge channels in void creating effective partial discharge area. IEEE Trans. Dielectr. Electr. Insul. 25 (6), 2220–2228. https://doi.org/10.1109/TDEI.2018.007426.
Forssen, C., Edin, H., 2008. Partial discharges in a cavity at variable applied frequency part 2: measurements and modeling. IEEE Trans. Dielectr. Electr. Insul. 15 (6), 1610–1616. https://doi.org/10.1109/TDEI.2008.4712664.
Gouda, O.E., ElFarskoury, A.A., Elsinnary, A.R., Farag, A.A., 2018. Investigating the effect of cavity size within medium-voltage power cable on partial discharge behaviour. IET Gener., Transm. Distrib. 12 (5), 1190–1197. https://doi.org/10.1049/iet-gtd.2017.1012.
Gross, D.W., 2018. Void and surface partial discharge pattern properties. In: 2018 International Conference on Diagnostics in Electrical Engineering (Diagnostika), Pilsen, Czech Republic, pp. 1–4. https://doi.org/10.1109/DIAGNOSTIKA.2018.8526142.
Haţiegan, C., Padureanu, I., Jurcu, M.R., Biriescu, M., Răduca, M., Dilertea, F., 2016. The evaluation of the insulation performances of the stator coil for the high power vertical synchronous hydro-generators by monitoring the level of partial discharges. Electr. Eng. 99 (3), 1013–1020. https://doi.org/10.1007/s00202-016-0471-5.
He, M., Hao, M., Chen, G., Chen, X., Li, W., Zhang, C., Wang, H., Zhou, M., Lei, X., 2018. Numerical modelling on partial discharge in HVDC XLPE cable. COMPEL - Int. J. Comput. Math. Electr. Electron. Eng. 37 (2), 986–999. https://doi.org/10.1108/COMPEL-07-2017-0297.
Hermansyah, M., Montanari, G.C., Seri, P., Suwarno, 2018. Investigating Partial Discharge Behaviour and Extracting Diagnostic Markers for Partial Discharge Aging of Type I Insulating Materials, 2018 Condition Monitoring and Diagnosis (CMD), Perth, WA, pp. 1–4. https://doi.org/10.1109/CMD.2018.8535668.
Hikita, M., Kozako, M., Takada, H., Higashiyama, M., Hirose, T., Nakamura, S., Umemura, T., 2010. Partial discharge phenomena in artificial cavity in epoxy cast resin insulation system. IEEE Int'l. Sympos. Electr. Insul. 1–5. https://doi.org/10.1109/ELINSL.2010.5549549.
Höfer, L., Berger, K.J., 2018. Partial Discharges under DC Voltage Stress Simulation and Measurement, 2018 IEEE International Conference on High Voltage Engineering and Application (ICHVE). ATHENS, Greece, pp. 1–4. https://doi.org/10.1109/ICHVE.2018.8641938.
Hussain, M.R., Refaat, S.S., Abu-Rub, H., 2021. Overview and partial discharge analysis of power transformers: a literature review. IEEE Access 9, 64587–64605. https://doi.org/10.1109/ACCESS.2021.3075288, 2021.
Iddrissu, I., Rowland, S.M., Zheng, H., Lv, Z., Schurch, R., 2018. Electrical tree growth and partial discharge in epoxy resin under combined AC and DC voltage waveforms. IEEE Trans. Dielectr. Electr. Insul. 25 (6), 2183–2190. https://doi.org/10.1109/TDEI.2018.007310.
Illias, H.A., Chen, G., Bakar, A.H.A., Mokhlis, H., Tunio, M.A., 2013. Partial discharges within two spherical voids in an epoxy resin. J. Phys. D Appl. Phys. 46 (33), 335301 https://doi.org/10.1088/0022-3727/46/33/335301.
Illias, H.A., Chen, G., Lewin, P.L., 2011a. Partial discharge behavior within a spherical cavity in a solid dielectric material as a function of frequency and amplitude of the applied voltage. IEEE Trans. Dielectr. Electr. Insul. 18 (2), 432–443. https://doi.org/10.1109/TDEI.2011.5739447.
Illias, H.A., Chen, G., Lewin, P.L., 2017. Comparison between three-capacitance, analytical-based and finite element analysis partial discharge models in condition monitoring. IEEE Trans. Dielectr. Electr. Insul. 24 (1), 99–109. https://doi.org/10.1109/TDEI.2016.005971.
Illias, H.A., Tunio, M.A., Abu Bakar, A.H.A., Mokhlis, H., Chen, G., 2014. Partial discharge behaviours within a void-dielectric system under square waveform applied voltage stress. IET Sci. Meas. Technol. 8 (2), 81–88. https://doi.org/10.1049/iet-smt.2013.0018.
Illias, H.A., Tunio, M.A., Mokhlis, H., Chen, G., Bakar, A.H.A., 2015. Determination of partial discharge time lag in void using physical model approach. IEEE Trans. Dielectr. Electr. Insul. 22 (1), 463–471. https://doi.org/10.1109/TDEI.2014.004618.
Illias, H., Chen, G., Lewin, P.L., 2011b. The influence of spherical cavity surface charge distribution on the sequence of partial discharge events. J. Phys. D Appl. Phys. 44 (24), 1–15. https://doi.org/10.1088/0022-3727/44/24/245202.
Jia, Y., Zhu, Y., 2018. Partial discharge pattern recognition using variable predictive model-based class discrimination with kernel partial least squares regression. IET Sci. Meas. Technol. 12 (3), 360–367. https://doi.org/10.1049/iet-smt.2017.0345.
Joseph, J., Mohan, S., Krishnan, S.T., 2019. Numerical modelling, simulation and experimental validation of partial discharge in cross-linked polyethylene cables. IET Sci. Meas. Technol. 13 (2), 309–317. https://doi.org/10.1049/iet-smt.2018.5248.
Kai, W., Okamoto, T., Suzuoki, Y., 2007. Effects of discharge area and surface conductivity on partial discharge behavior in voids under square voltages. IEEE Trans. Dielectr. Electr. Insul. 14 (2), 461–470. https://doi.org/10.1109/TDEI.2007.344627.
Kai, W., Yasuo, S., Dissado, L.A., 2004. The contribution of discharge area variation to partial discharge patterns in disc-voids. J. Phys. D Appl. Phys. 37 (13), 1815–1823. https://doi.org/10.1088/0022-3727/37/13/013.
Kaneiwa, H., Suzuoki, Y., Mizutani, T., 2000. Partial discharge characteristics and tree inception in artificial simulated tree channels. IEEE Trans. Dielectr. Electr. Insul. 7 (6), 843–848. https://doi.org/10.1109/94.891998.
Kim, C., Kondo, T., Mizutani, T., 2004. Change in PD pattern with aging. IEEE Trans. Dielectr. Electr. Insul. 11 (1), 13–18. https://doi.org/10.1109/TDEI.2004.1266311.
Kim, D., Siada, A.A., 2018. Partial Discharge Analysis On-Site in Various High Voltage Apparatus, 2018 Condition Monitoring and Diagnosis (CMD), Perth, WA, pp. 1–6. https://doi.org/10.1109/CMD.2018.8535987.
Lemke, E., 2016. Using a field probe to study the mechanism of partial discharges in very small air gaps under direct voltage. IEEE Electr. Insul. Mag. 32 (4), 43–51. https://doi.org/10.1109/MEI.2016.7528989.
Li, K., Javed, H., Zhang, G., Plesca, A.T., 2017a. Analysis of air decomposition by-products under four kinds of partial discharge defects. IEEE Trans. Dielectr. Electr. Insul. 24 (6), 3713–3721. https://doi.org/10.1109/TDEI.2017.006706.
Li, P., Zhou, W., Yang, S., Liu, Y., Tian, Y., Wang, Y., 2017b. A novel method for separating and locating multiple partial discharge sources in a substation. Sensors 17 (2), 247. https://doi.org/10.3390/s17020247.
Liu, M., Liu, Y., Li, Y., Zheng, P., Rui, H., 2017. Growth and partial discharge characteristics of electrical tree in XLPE under AC-DC composite voltage. IEEE Trans. Dielectr. Electr. Insul. 24 (4), 2282–2290. https://doi.org/10.1109/TDEI.2017.006537.
Liu, T., Li, Q., Huang, X., Lu, Y., Asif, M., Wang, Z., 2018. Partial discharge behavior and ground insulation life expectancy under different voltage frequencies. IEEE Trans. Dielectr. Electr. Insul. 25 (2), 603–613. https://doi.org/10.1109/TDEI.2018.006810.
Lv, Z., Rowland, S.M., Chen, S., Zheng, H., Iddrissu, I., 2017. Evolution of partial discharges during early tree propagation in epoxy resin. IEEE Trans. Dielectr. Electr. Insul. 24 (5), 2995–3003. https://doi.org/10.1109/TDEI.2017.006731.
Lv, Z., Rowland, S.M., Chen, S., Zheng, H., Wu, K., 2018. Modelling of partial discharge characteristics in electrical tree channels: estimating the PD inception and extinction voltages. IEEE Trans. Dielectr. Electr. Insul. 25 (5), 1999–2010. https://doi.org/10.1109/TDEI.2018.007175.
Madhar, S.A., Mor, A.R., Mraz, P., Ross, R., 2021. Study of DC partial discharge on dielectric surfaces: mechanism, patterns and similarities to AC. Int. J. Electr. Power Energy Syst. 126 (Part B), 106600 https://doi.org/10.1016/j.ijepes.2020.106600.
Majidi, M., Fadali, M.S., Etezadi-Amoli, M., Oskuoee, M., 2015. Partial discharge pattern recognition via sparse representation and ANN. IEEE Trans. Dielectr. Electr. Insul. 22 (2), 1061–1070. https://doi.org/10.1109/TDEI.2015.7076807.
McAllister, I.W., Pedersen, A., 1981. Corona-onset field-strength calculations and the equivalent radius concept. Arch. Elektrotechnik 64 (1), 43–48. https://doi.org/10.1007/BF01476309.
Mendiola, J.Y., Vacio, R.J., Colin, J.Á., Jimenez, J.T., Godoy, F.F., 2017. Analysis of insulating material of xlpe cables considering innovative patterns of partial discharges. Math. Probl Eng. 2017, 1–10. https://doi.org/10.1155/2017/2379418.
Mor, A.R., Heredia, L.C.C., 2018. Practical frequency response characterization of a test circuit for partial discharge measurements. IEEE Trans. Dielectr. Electr. Insul. 25 (4), 1535–1544. https://doi.org/10.1109/TDEI.2018.006884.
Niasar, M.G., Wang, X., Kiiza, R.C., 2021. Review of partial discharge activity considering very-low frequency and damped applied voltage. Energies 14 (2), 440. https://doi.org/10.3390/en14020440.
Nijdam, S., van de Wetering, F.M.J.H., Blanc, R., Veldhuizen, E.M.V., Ebert, U., 2010. Probing photo-ionization: experiments on positive streamers in pure gases and mixtures. J. Phys. Appl. Phys. 43 (14) https://doi.org/10.1088/0022-3727/43/14/145204, 2010.
Noguchi, S., Nakamichi, M., Oguni, K., 2020. Proposal of finite element analysis method for dielectric breakdown based on Maxwell's equations. Comput. Methods Appl. Mech. Eng. 371, 113295 https://doi.org/10.1016/j.cma.2020.113295.
Pan, C., Meng, Y., Wu, K., Han, Z., Qin, K., Cheng, Y., 2011. Simulation of partial discharge sequences using fluid equations. J. Phys. Appl. Phys. 44 (25), 255201 https://doi.org/10.1088/0022-3727/44/25/255201.
Pan, C., Tang, J., Wu, K., 2016a. The effect of PD process on the accumulation of surface charges. IEEE Trans. Plasma Sci. 44 (11), 2545–2552. https://doi.org/10.1109/TPS.2016.2581309.
Pan, C., Wu, K., Chen, G., Gao, Y., Florkowski, M., Lv, Z., Tang, J., 2020. Understanding partial discharge behavior from the memory effect induced by residual charges: a review. IEEE Trans. Dielectr. Electr. Insul. 27 (6), 1951–1965. https://doi.org/10.1109/TDEI.2020.008960.
Pan, C., Wu, K., Du, Y., Meng, Y., Cheng, Y., Tang, J., 2016b. The effect of surface charge decay on the variation of partial discharge location. IEEE Trans. Dielectr. Electr. Insul. 23 (4), 2241–2249. https://doi.org/10.1109/TDEI.2016.7556500.
Pedersen, A., Crichton, G., McAllister, I.W., 1993. PD-related stresses in the bulk dielectric and their evaluation. In: Proceedings of IEEE Conference on Electrical

Insulation and Dielectric Phenomena - (CEIDP '93), pp. 474–480. https://doi.org/10.1109/CEIDP.1993.378927.
Pedersen, A., Crichton, G.C., McAllister, I.W., 1991. The theory and measurement of partial discharge transients. Electr. Insul. IEEE Trans. Electr. Insul. 26 (3), 487–497. https://doi.org/10.1109/14.85121.
Renforth, L.A., Giussani, R., Mendiola, M.T., Dodd, L., 2019. Online partial discharge insulation condition monitoring of complete high-voltage networks. IEEE Trans. Ind. Appl. 55 (1), 1021–1029. https://doi.org/10.1109/TIA.2018.2866983.
Riande, E., Calleja, R.D., 2013. Electrical properties of polymers. Mater. Prop. Test. https://doi.org/10.1002/9781118436707.hmse039.
Rodríguez-Serna, J.M., Albarracín-Sánchez, R., Dong, M., Ren, M., 2020. Computer simulation of partial discharges in voids inside epoxy resins using three-capacitance and analytical models. Polymers 12 (1), 77. https://doi.org/10.3390/polym12010077.
Romano, P., Presti, G., Imburgia, A., Candela, R., 2018. A new approach to partial discharge detection under DC voltage. IEEE Electr. Insul. Mag. 34 (4), 32–41. https://doi.org/10.1109/MEI.2018.8430041.
Schifani, R., Candela, R., Romano, P., 2001. On PD mechanisms at high temperature in voids included in an epoxy resin. IEEE Trans. Dielectr. Electr. Insul. 8 (4), 589–597. https://doi.org/10.1109/94.946711.
Sefl, O., Prochazka, R., 2022. Investigation of supraharmonics influence on partial discharge activity using an internal cavity sample. Int. J. Electr. Power Energy Syst. 134 https://doi.org/10.1016/j.ijepes.2021.107440.
Seghir, T., Mahi, D., Lebey, T., Malec, D., 2006. Analysis of the electric field and the potential distribution in cavities inside solid insulating electrical materials. Proc. COMSOL Users Confer. Paris 9.
Shcherbanev, S.A., Nadinov, I.U., Auvray, P., Starikovskaia, S.M., Pancheshnyi, S., Herrmann, L.G., 2016. Emission spectroscopy of partial discharges in air-filled voids in unfilled epoxy. IEEE Trans. Plasma Sci. 44 (7), 1219–1227. https://doi.org/10.1109/TPS.2016.2576560.
Singh, S., Serdyuk, Y.V., Gubanski, S.M., 2018. Simulations of electrical discharges in air using stabilized drift-diffusion model. IEEE Trans. Plasma Sci. 46 (8), 3031–3039. https://doi.org/10.1109/TPS.2018.2850803.
Suzuoki, Y., Komori, F., Mizutani, T., 1996. Partial discharges due to electrical treeing in polymers: phase-resolved and time-sequence observation and analysis. J. Phys. D Appl. Phys. 29 (11), 2922–2931. https://doi.org/10.1088/0022-3727/29/11/028.
Takabayashi, K., Nakane, R., Okubo, H., Kato, K., 2018. High voltage DC partial discharge and flashover characteristics with surface charging on solid insulators in air. IEEE Electr. Insul. Mag. 34 (5), 18–26. https://doi.org/10.1109/MEI.2018.8445431.
Toader, M., Mariana, D., 2000. Electrical insulation study using partial discharge model. In: 2000 10th Mediterranean Electrotechnical Conference. Information Technology and Electrotechnology for the Mediterranean Countries. Proceedings. MeleCon 2000 (Cat. No.00CH37099), vol. 3, pp. 1060–1063. https://doi.org/10.1109/MELCON.2000.879717.
Venger, R., Tmenova, T., Valensi, F., Veklich, A., Cressault, Y., Boretskij, V., 2017. Detailed investigation of the electric discharge plasma between copper electrodes immersed into water. Atoms 5 (4), 40. https://doi.org/10.3390/atoms5040040.
Villa, A., Barbieri, L., Gondola, M., Leon-Garzon, A.R., Malgesini, R., 2017. A PDE-based partial discharge simulator. J. Comput. Phys. 345, 687–705. https://doi.org/10.1016/j.jcp.2017.05.045.
Wang, C., Huang, X., Lu, K., Li, G., Zhu, H., Wang, J., Wang, C., Dai, Z., Fang, L., Song, Y., 2017. Influence of void defects on partial discharge behavior of superconducting busbar insulation. Fusion Eng. Des. 119, 29–34. https://doi.org/10.1016/j.fusengdes.2017.04.117.
Xu, Y., Burgos, R., Boroyevich, D., 2017. Insulation design and evaluation via partial discharge (PD) test for power electronics application. In: 2017 IEEE Electric Ship Technologies Symposium (ESTS), Arlington, VA, pp. 394–400. https://doi.org/10.1109/ESTS.2017.8069312.
Yang, M.X., Yang, F., Lee, S., 2021. Dielectric breakdown sizes of conducting plates. IMA J. Appl. Math. 86 (3), 502–513. https://doi.org/10.1093/imamat/hxab013.
Yousfi, B., Lefkaier, I.K., 2018. Simulation of partial discharges initiation in voids in medium voltage cables insulators. IEEE Trans. Dielectr. Electr. Insul. 25 (3), 892–899. https://doi.org/10.1109/TDEI.2018.006790.
Zeng, F., Lei, Z., Yang, X., Tang, J., Yao, Q., Miao, Y., 2019. Evaluating DC partial discharge with SF6 decomposition characteristics. IEEE Trans. Power Deliv. 34 (4), 1383–1392. https://doi.org/10.1109/TPWRD.2019.2900508.